

Steady-State Kinetics and Tryptophan Fluorescence Properties of Halohydrin Dehalogenase from *Agrobacterium radiobacter*. Roles of W139 and W249 in the Active Site and Halide-Induced Conformational Change[†]

Lixia Tang, Annet E. J. van Merode, Jeffrey H. Lutje Spelberg, Marco W. Fraaije, and Dick B. Janssen*

Laboratory of Biochemistry, Groningen Biomolecular Sciences and Biotechnology Institute, University of Groningen, Nijenborgh 4, 9747 AG Groningen, The Netherlands

Received June 2, 2003; Revised Manuscript Received September 3, 2003

ABSTRACT: Halohydrin dehalogenase (HheC) from *Agrobacterium radiobacter* AD1 is a homotetrameric protein containing four tryptophan residues per subunit. The fluorescence properties of the enzyme are strongly influenced by halide binding. To examine the role of the tryptophans (W139, W192, W238, and W249) in halide binding and catalysis, they were individually mutated to a phenylalanine. All mutations, except for W238F, influenced the enzymatic properties. Mutating W192 to phenylalanine inactivated the enzyme and led to dissociation into dimers and monomers. In the structure of HheC, residue W139 and residue W249 from the opposite subunit are close to the active site of the enzyme. Substitution of W139 mainly affected K_m values with all tested substrates and reduced the enantioselectivity for *p*-nitro-2-bromo-1-phenylethanol. Replacing W249 increased both k_{cat} and K_m values with all tested substrates except for the (*S*)-enantiomer of *p*-nitro-2-bromo-1-phenylethanol, for which k_{cat} was 3-fold decreased, resulting in a 6-fold increase of the enantioselectivity. Fluorescence measurements revealed that in the ligand-free state the intrinsic protein fluorescence of mutant W139F is higher than that of the wild-type enzyme, while the fluorescence intensity of mutants W238F and W249F was lower. The fluorescence intensities of the W238F and W249F enzymes were increased when they were unfolded or when bromide was added, whereas the fluorescence of mutant W139F was not increased by unfolding or addition of bromide. These results demonstrate that the fluorescence of residues W238 and W249 is partially quenched in the folded ligand-free state, and that W139 is completely quenched and acts as an energy acceptor for the other tryptophan residues as well. Changes of the maximum fluorescence emission wavelength of the HheC variants and the results of acrylamide quenching experiments confirmed that bromide binding induces a local conformational change around the active site, resulting in residue W139 and the quencher group being separated.

Halohydrin dehalogenases catalyze the reversible intramolecular nucleophilic displacement of a halogen by a hydroxyl group in vicinal halohydrins, producing the corresponding epoxides. This is a key detoxification reaction in the degradation of various halogenated compounds. So far, only a few halohydrin dehalogenases have been characterized (1–6). We have recently cloned and expressed in *E. coli* BL21-DE3 the halohydrin dehalogenase gene (*hheC*) from *Agrobacterium radiobacter* AD1, a Gram-negative bacterium capable of using epichlorohydrin and chloropropanols as the sole carbon and energy source (3, 7). The enzyme HheC¹ is a homotetramer with 28 kDa subunits. HheC exhibits high enantioselectivity toward some aromatic halohydrins, and it can be used to produce enantiomerically pure aromatic halohydrins, epoxides, and diols using a tandem reaction with

an epoxide hydrolase obtained from the same organism (8, 9). The enzyme also accepts alternative nucleophiles in the reverse (epoxide ring-opening) reaction, such as azide (9).

HheC shows significant sequence similarity with the short-chain dehydrogenase/reductase (SDR) protein family (3). This allowed a prediction of the global three-dimensional structure of HheC using protein structures of the SDR family as templates. Furthermore, site-directed mutagenesis studies have identified three residues, Ser132, Tyr145, and Arg149, which are involved in catalysis (Figure 1). The experimental structure, which was solved recently, confirmed these propositions, and also revealed the presence of a halide-binding site (10). However, a structure of the halide-free enzyme is not available. The structure shows that two of the four tryptophans of HheC, W139 and W249 (from the opposite 2-fold symmetry related subunit), are close to the active site, whereas W192 and W238 are less close. Moreover, tryptophan residues are found to be located in the active site and play a role in substrate binding in some other dehalogenases, as well as in epoxide hydrolases and SDR proteins (11–18). Nardini et al. reported that the substrate-binding site of epoxide hydrolase from *A. radio-*

[†] This work was supported by Grant QLK3-2000-00426 from the EU.

* To whom correspondence should be addressed. Phone: (+31) 50-3634209. Fax: (+31) 50-3634165. E-mail: D.B.Janssen@chem.rug.nl.

¹ Abbreviations: HheC, halohydrin dehalogenase; PNSHH, *p*-nitro-2-bromo-1-phenylethanol; SDR, short-chain dehydrogenase/reductase; PNSO, *p*-nitrostyrene oxide; K_{sv} , Stern–Volmer quenching constant; NATA, *N*-acetyltryptophanamide; DEPC, diethyl pyrocarbonate.

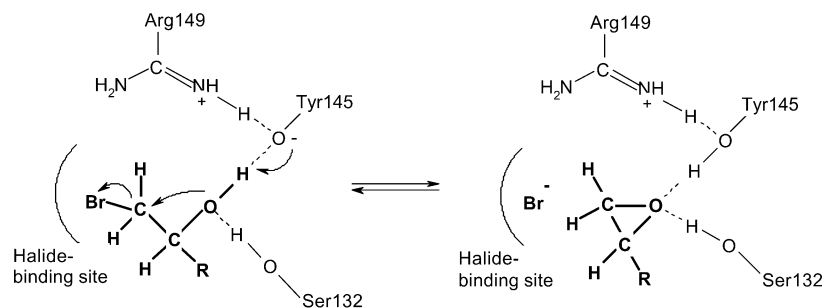


FIGURE 1: Proposed reaction mechanism of halohydrin dehalogenase from *A. radiobacter* AD1 (HheC).

bacter AD1 is lined by two tryptophan residues (14). In haloalkane dehalogenase, W125 and W175 play a role in halogen and halide binding and are important for catalysis (16). It has been shown that these active site tryptophans can be used as fluorescent probes to study substrate binding and structural changes that occur upon ligand binding.

In the present study, we used site-directed mutagenesis to investigate the role of tryptophan residues in substrate binding and protein fluorescence of HheC by constructing four tryptophan mutants (W139F, W192F, W238F, and W249F) and by measuring their catalytic and fluorescence properties.

MATERIALS AND METHODS

Materials. Standard chemicals and biochemicals were obtained from Sigma, Acros, Merck, and Aldrich. Both enantiomers of *p*-nitro-2-bromo-1-phenylethanol (PNSHH) were synthesized as described by Westkaemper and Hanzlik (19). The enantiomers of PNSHH were separated by preparative HPLC using an analytical Chiralpak AS column (5 mm inside diameter) with hexane/2-propanol (95:5) as eluent (flow rate 1.3 mL/min), which yielded product of at least 98% enantiopurity. The retention times of individual enantiomers are as follows: (*R*)-PNSHH, 25.5 min; (*S*)-PNSHH, 28.9 min. Oligonucleotide primers were from Sigma Genosys.

Mutagenesis. The previously constructed plasmid pGEF-HheC (3), containing the *A. radiobacter hheC* gene (accession number AF397296), was used as the template for mutagenesis. Mutant genes were constructed using the QuikChange site-directed mutagenesis kit of Stratagene (LaJolla, Ca) following the recommendations of the manufacturer. W139 was mutated to Phe with primer 5'-CCC-TTCGGGCCT7TTAAGGAACCTTCTACC. W192 was changed to Phe with primer 5'-CCCCACAGAACCGTT-TAAACGAATCCAGA. Primers 5'-CGGCCAGGTGT-TC7TTTTGGCCGGCGGAT and 5'-AATGATC-GAGCGT7TTCTTGGTATGCCCCGA were used to obtain mutants W238F and W249F, respectively. Successful mutagenesis was confirmed by sequence analysis.

Expression, Purification, and Enzyme Assays. Wild-type and mutant HheC enzymes were expressed in *E. coli* BL-21(DE3) and purified by using Q Sepharose (130 mL, Pharmacia Biotech) and Resource Phe (40 mL, Pharmacia Biotech) columns as described before (20). All buffers contained 10% glycerol and 1 mM β -mercaptoethanol to improve the stability of the enzyme (21). The enzyme could be stored at -70°C for at least three months without significant loss of activity.

After purification the halohydrin dehalogenase activity was determined by monitoring bromide liberation at 30°C using 5 mM 2-bromoethanol in 50 mM Tris/ SO_4 buffer (pH 8.0) (22). The concentration of protein was determined by measuring the absorbance at 280 nm. The extinction coefficient of HheC was calculated by using the program Dnstar (wild type, $\epsilon_{280} = 35920 \text{ cm}^{-1}\cdot\text{M}^{-1}$; mutants, $\epsilon_{280} = 30230 \text{ cm}^{-1}\cdot\text{M}^{-1}$).

Circular Dichroism Spectroscopy. Far-UV CD spectra were recorded on an AVIV model 62A DS circular dichroism spectrometer. The CD spectra were recorded from 190 to 250 nm using a 0.1-cm cuvette containing 0.1 mg/mL halohydrin dehalogenase (5 mM potassium phosphate, pH 7.5) at 25°C . Each spectrum shown represents the average of five scans and was corrected for the absorbance caused by the buffer.

Steady-State Kinetics Measurements. Initial velocities were measured at 30°C on a Perkin-Elmer Lambda Bio 10 UV/vis spectrometer by monitoring the absorbance change at 310 nm using the chromogenic substrate *p*-nitro-2-bromo-1-phenylethanol in 50 mM Tris/ SO_4 buffer (pH 7.5) ($\epsilon_{\text{PNSHH}} = 3100 \text{ cm}^{-1}\cdot\text{M}^{-1}$; $\epsilon_{\text{PNSO}} = 4289 \text{ cm}^{-1}\cdot\text{M}^{-1}$) (23). Initial rates were determined from the initial linear part of the reaction progress curves. The steady-state initial velocity pattern in the absence of products was obtained by varying the concentration of substrate. Kinetic data were fitted with the Michaelis-Menten equation using Sigmaplot 2000 to obtain the steady-state kinetic parameters. For 1-chloro-2-methyl-2-propanol, the initial velocity was determined by monitoring halide liberation (22). All k_{cat} values are defined as per monomer.

Fluorescence Measurements. Steady-state fluorescence measurements were performed on a Fluorolog-3 spectrofluorometer at 30°C . The excitation wavelength was 290 nm, and emission spectra were recorded in the range of 300–450 nm. Immediately prior to the experiment the enzyme was diluted to a desired concentration.

For the steady-state substrate binding experiments, 0.03 mg/mL protein solutions were used. Halide and epoxides were added from freshly prepared stock solutions in 50 mM Tris/sulfate buffer (pH 8.0) containing 1 mM β -mercaptoethanol. The change in fluorescence was corrected for dilution, which did not exceed 10%. Substrate binding was analyzed from the relative change of the fluorescence intensity at λ_{Emax} (ΔF) at varying substrate concentrations. Apparent steady-state dissociation constants were obtained by nonlinear regression fitting of eq 1 using Sigmaplot 2000. In this equation, $[S]$ is the concentration of halide or epoxides, K_d is the apparent dissociation constant, and f_a is

Table 1: Steady-state Kinetic Parameters of Wild-Type and Mutant HheC^a

enzyme	1-chloro-2-methyl-2-propanol			(R)-PNSHH			(S)-PNSHH			E
	K_m (mM)	k_{cat} (s ⁻¹)	k_{cat}/K_m (s ⁻¹ ·M ⁻¹)	K_m (mM)	k_{cat} (s ⁻¹)	k_{cat}/K_m (s ⁻¹ ·M ⁻¹)	K_m (mM)	k_{cat} (s ⁻¹)	k_{cat}/K_m (s ⁻¹ ·M ⁻¹)	
WT	0.26 ± 0.06	68 ± 5	2.6 × 10 ⁵	0.009 ± 0.003	22 ± 1	2.4 × 10 ⁶	0.43 ± 0.05	7 ± 1	1.6 × 10 ⁴	150
W139F	6.7 ± 0.76	44 ± 3	6.5 × 10 ³	0.15 ± 0.04	38 ± 5	2.5 × 10 ⁵	0.06 ± 0.01	13 ± 1	2.1 × 10 ⁵	1.2
W238F	0.11 ± 0.02	74 ± 2	6.5 × 10 ⁵	0.007 ± 0.003	21 ± 1	3.0 × 10 ⁶	0.23 ± 0.03	4 ± 0.2	1.7 × 10 ⁴	176
W249F	2.5 ± 0.59	80 ± 7	3.2 × 10 ⁴	0.050 ± 0.01	170 ± 13	3.3 × 10 ⁶	0.61 ± 0.08	2.3 ± 0.3	3.8 × 10 ³	900

^a No activity was detected for mutant W192F.

the relative change of the fluorescence intensity at $[S] \gg K_d$.

$$\Delta F = f_a[S]/([S] + K_d) \quad (1)$$

Fluorescence emission spectra and λ_{Emax} were measured at a protein concentration of 0.1 mg/mL in the absence and presence of bromide. The emission spectra of all HheC variants were also measured in the presence of 7.8 M urea.

The quantum yield of protein fluorescence was determined in 50 mM Tris/SO₄ buffer (pH 8.0) at 30 °C using *N*-acetyltryptophanamide (NATA) as a standard, $\Phi = 0.14$ (24). The excitation wavelength was 290 nm, and the emission was measured from 300 to 450 nm with a 2-nm band-pass for excitation and a 5-nm band-pass for emission. The protein concentration was adjusted to give an absorbance at 290 nm between 0.05 and 0.1.

For fluorescence quenching experiments with the collisional quencher acrylamide, a protein concentration of 0.03 mg/mL was used. Fluorescence was measured after aliquots of freshly prepared 8 M acrylamide were added to the protein solution either in the presence or in the absence of substrate. The acrylamide quenching data were fitted to the Stern–Volmer equation (eq 2) (25). F_0 and F are the fluorescence intensities at an appropriate emission wavelength in the absence and presence of acrylamide, respectively. $[Q]$ is the concentration of quencher, and K_{sv} is the Stern–Volmer quenching constant.

$$F_0/F = 1 + K_{sv}[Q] \quad (2)$$

Chemical Modification with Diethyl Pyrocarbonate. A stock solution (600 mM) of diethyl pyrocarbonate (DEPC) was freshly prepared in cold absolute ethanol immediately before use. The modification reactions were initiated by the addition of DEPC (final concentration 3 mM) to the enzyme solution (0.2 mg/mL) in 50 mM Tris/SO₄ at 25 °C. Samples were taken in time, and the modification of histidine residues was followed by analyzing the difference UV absorbance spectra with a Perkin-Elmer Lambda Bio 10 UV/vis spectrometer. The formation of *N*-carbethoxyhistidine was calculated from the increase in absorbance at 240 nm using an extinction coefficient of 3200 M⁻¹·cm⁻¹ (26).

RESULTS

Properties of Tryptophan Mutants. To probe the role of individual tryptophan residues, all four tryptophans were individually replaced by phenylalanines. The mutants W139F, W192F, W238F, and W249F were expressed and purified as described previously for the wild-type enzyme (20). All mutants were produced as soluble proteins up to a level of 30% of the total protein in cell-free extract in *E. coli* BL21-

(DE3), and the mutated proteins were isolated to a purity of about 95% as judged by SDS–PAGE.

Purified W192F halohydrin dehalogenase did not show significant activity with (R)-PNSHH, one of the best substrates of HheC in the ring-closure reaction (27). A crude cell-free extract of this mutant was also inactive, excluding the possibility that inactivation occurred during the purification procedure. The other three mutant enzymes showed significant activity (Table 1). To determine if the lack of activity of mutant W192F was caused by incorrect folding of the protein, the secondary structures of wild-type enzyme and the mutants were measured by far-UV circular dichroism spectroscopy. All mutant proteins, including W192F, displayed spectra similar to that of the wild-type enzyme (data not shown), indicating that the mutations had no significant effect on the secondary structure of proteins. In a recent study, it was reported that wild-type HheC is only active as a homotetramer (21). Therefore, the oligomeric state of all mutants was probed by gel filtration. All mutants appeared to be present as tetramers except for mutant W192F. Under the conditions used, this mutant enzyme was composed of about 90% dimers and 10% monomers (data not shown). This suggests that the local structural change due to the W192F mutation results in protein dissociation, which might also be the reason for enzyme inactivation. Therefore, mutant W192F was not studied further.

The steady-state kinetic parameters and enantioselectivity of the active mutants were examined using a nonchiral aliphatic substrate (1-chloro-2-methyl-2-propanol) and two chiral aromatic substrates ((R)- and (S)-PNSHH) (Table 1). It was found that mutating W238 to a phenylalanine had a relatively small effect on the K_m and k_{cat} values for all three substrates. Thus, the ratios of k_{cat}/K_m for mutant W238F and wild-type HheC with the enantiomers of PNSHH are similar, and the enantioselectivity was maintained. Substitution of W139 or W249 by phenylalanine, which are located close to the active site (10), drastically altered the kinetics of the enzyme. The W139F mutation mainly resulted in different K_m values, while the k_{cat} values were affected to a lesser extent. Mutation of W139 caused a 26-fold increase in K_m for 1-chloro-2-methyl-2-propanol and a 17-fold increase in K_m for (R)-PNSHH, while it resulted in a 7.2-fold decrease in K_m for (S)-PNSHH. The W139F mutation caused opposite effects on the k_{cat}/K_m values for the (R)- and the (S)-enantiomers of PNSHH (9.6-fold decrease and 13-fold increase, respectively), resulting in a complete loss of enantioselectivity of the enzyme for PNSHH.

Replacing W249 also resulted in changes of the K_m and k_{cat} values. The W249F mutant exhibited a 9.6-fold increase in K_m for 1-chloro-2-methyl-2-propanol and a 5.6-fold increase in K_m for (R)-PNSHH, while K_m for (S)-PNSHH

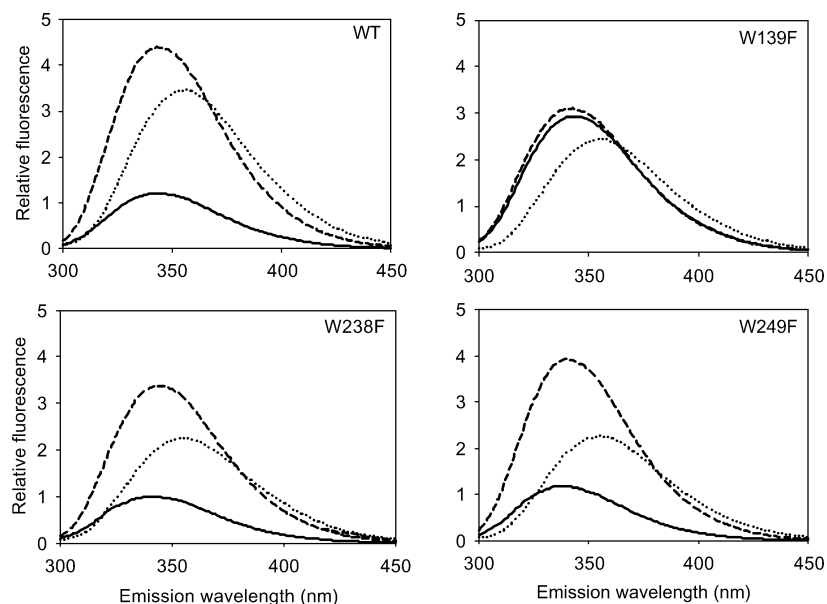


FIGURE 2: Intrinsic fluorescence emission spectra of wild-type and mutant HheC. The spectra were determined in the presence (···) and absence (—) of 7.8 M urea. The effect of substrate on the emission spectra was also investigated in the presence of 20 mM bromide (---). The emission spectra were recorded at $\lambda_{\text{Ex}} = 290$ nm using 0.1 mg/mL protein solutions prepared in 50 mM Tris/sulfate buffer (pH 8.0) containing 1 mM β -mercaptoethanol.

was only slightly affected. The mutation resulted in a small effect on the k_{cat} value for the aliphatic substrate, while there was a large effect on the rate of conversion of the aromatic substrates (7.7-fold increase with (*R*)-PNSHH and 3-fold decrease with (*S*)-PNSHH). Consequently, the $k_{\text{cat}}/K_{\text{m}}$ values were 1.4-fold increased for (*R*)-PNSHH and 4.2-fold decreased for (*S*)-PNSHH, resulting in a 6-fold increase in enantioselectivity compared with that of wild-type HheC. These results suggest that residues W139 and W249 can interact with substrate, which is in agreement with the structural data, which indicate that the indole side chains of W139 and W249 line a binding pocket for the aromatic groups of (*R*)-styrene oxide and (*R*)-1-*p*-nitrophenyl-2-azidoethanol (10). Moreover, it appeared that the mutations of W139 and W249 had opposite effects on the enantioselectivity toward PNSHH.

Steady-State Fluorescence Properties of Wild-Type HheC and the Tryptophan Mutants. The three active tryptophan mutants were used to study the role of individual tryptophan residues in protein fluorescence (Figure 2). The emission spectra of the ligand-free wild-type enzyme and mutant showed a broad fluorescence maximum at 339–342 nm (Table 3), which indicates that the average microenvironment of the indole side chains of tryptophans in HheC is relatively hydrophobic (28). The microenvironment of W249 seems to be more polar than that of the other two residues as a 3-nm blue shift was observed when W249 was replaced by a phenylalanine.

Inspection of the fluorescence intensities of the native ligand-free enzymes revealed that the intrinsic protein fluorescence increased when W139 was replaced by a phenylalanine, whereas the fluorescence intensity of mutants W238F and W249F was somewhat lower than that of the wild-type enzyme (Table 2). This indicates either that W139 reduces the total fluorescence intensity in the wild-type enzyme or that there is a large change in the environment of the other three tryptophans when W139 is replaced by a phenylalanine. The latter explanation is unlikely since

Table 2: Relative Fluorescence Intensity (FI) and the Fluorescence Quantum Yield (Φ) of HheC Variants

enzyme	relative fluorescence intensity (%)			Φ
	ligand-free native state	ligand-free unfolded state	with bromide (20 mM)	
WT ^a	100	280	360	0.05
W139F	250	210	260	0.13
W238F	85	195	250	0.07
W249F	98	195	300	0.06

^a The fluorescence emission maximum intensity of wild-type HheC in the ligand-free native state was set as 100%.

mutating W139 did not show a significant effect on the emission wavelength maximum of the enzyme. The fluorescence of W238 and W249 in the wild-type enzyme appears to be partially quenched since the decrease of fluorescence intensity of W238F and W249F compared to the wild-type enzyme was much less than proportional. This could be due to energy transfer to W139 or to other neighboring residues. Therefore, W192 might have a relatively high contribution to the total protein fluorescence.

The fluorescence quantum yields of active mutants and wild-type HheC were measured in the absence of any ligands (Table 2). The wild-type enzyme and mutants W238F and W249F possessed a similar low Φ value, while mutant W139F showed a high value. It is obvious that the quantum yield of the wild-type enzyme is not additive. This suggests a tryptophan–tryptophan energy-transfer mechanism.

To obtain more information about the microenvironment of the tryptophans, the fluorescence emission spectra of wild-type HheC and mutants W139F, W238F, and W249F were measured in the presence of 7.8 M urea (Figure 2). It was found that the emission maxima of the proteins were red shifted to 356–355 nm (Table 3), indicating that the proteins became unfolded. Upon unfolding in urea, wild-type HheC and mutants W238F and W249F displayed a large increase of fluorescence intensities, while only a small change of intensity was observed with mutant W139F (Table 2). These

Table 3: Emission Maxima (λ_{Emax}), Dissociation Constants (K_d), and Acrylamide Stern–Volmer Quenching Constants (K_{sv}) of Both Wild-Type and Mutant HheC^a

enzyme	λ_{Emax} (nm)		Cl [−]		Br [−]		I [−]		K_{sv}	
	folded	unfolded	K_d (mM)	λ_{Emax} (nm)	K_d (mM)	λ_{Emax} (nm)	K_d (mM)	λ_{Emax} (nm)	ligand-free native state	bromide (20 mM)
WT	342	356	4.1 ± 0.8	343	1.3 ± 0.2	343	1.2 ± 0.2	343	9.0	28.0
W139F	343	356	-	340	-	340	-	340	9.1	12.8
W238F	342	356	6.8 ± 1.4	344	1.4 ± 0.2	345	2.3 ± 0.5	345	11.6	38.6
W249F	339	355	7.6 ± 1.1	340	1.1 ± 0.2	340	2.1 ± 0.2	340	10.6	12.5

^a The K_d values are the average of two to four determinations. The plots from which the quenching constants were determined are shown in Figure 3. A dash indicates no significant change of fluorescence intensity was detected.

results again indicate that W139 plays a role in tryptophan fluorescence quenching in native HheC.

Effect of Substrate on Tryptophan Fluorescence Properties of HheC Variants. To probe the role of individual tryptophans in the halide-induced fluorescence enhancements, fluorescence emission spectra were measured in the presence of a saturating concentration of bromide (Figure 2). By comparison of the fluorescence intensity of HheC variants to that of the wild-type enzyme in the presence of 20 mM bromide (Table 2), it was found that residues W139, W238, and W249 contributed 28%, 30%, and 17%, respectively, of the total fluorescence intensity of wild-type HheC when bromide was bound. Therefore, W192 must contribute about 25% of the total fluorescence.

Upon adding bromide, a 3-nm blue shift of λ_{Emax} was observed for mutant W139F compared to mutant W139F in the ligand-free state, which shows that the average microenvironment of the remaining tryptophans W192, W238, and W249 became more hydrophobic upon bromide binding. However, this did not cause a remarkable increase of their fluorescence intensity. Thus, the large increase in fluorescence observed in the wild-type enzyme when bromide is added is not due to a change of the microenvironment of residues W192, W238, and W249, but it must be mainly due to a separation taking place between W139 and its quencher group.

When fluorescence emission maxima were measured in the presence of 20 mM bromide, a 3-nm blue shift of λ_{Emax} was observed for mutants W139F and W249F while a 2-nm red shift was found for mutant W238F in comparison to the λ_{Emax} value of bromide-bound wild-type HheC (Table 3). Thus, the local environment of W139 and W249 is relatively hydrophilic and that of W238 is somewhat more hydrophobic compared to the average microenvironment of the four tryptophans in ligand-bound HheC. This is consistent with the observation that W139 and W249 are more exposed to the solvent than residue W238 (10). A similar effect of the mutations on the emission maxima of HheC variants was observed with the other halide ions (Table 3).

The observation that the fluorescence intensity of HheC and the W238F and W249F mutants was increased upon halide binding suggests that tryptophan fluorescence can be used as a probe to determine halide dissociation constants (K_d). Accordingly, the K_d values for the halide of the active HheC variants, except for mutant W139F, were determined by fluorometric titration (Table 3). The wild-type HheC showed similar K_d values of around 1 mM for iodide and bromide, whereas the K_d value for chloride was about 3.5-fold higher. Moreover, it was found that wild-type HheC had a lower K_d value at lower pH. Mutants W238F and

W249F displayed dissociation constants with halides Cl[−], Br[−], and I[−] similar to those of the wild-type enzyme. Thus, the mutations had little effect on halide binding, although mutation of residue W249 influenced the kinetics of PNSHH conversion. For mutant W139F, it appeared that bromide still binds to the enzyme since an inhibition constant of 0.9 mM was found for bromide during the conversion of (R)-PNSHH, which is similar to that of the wild-type enzyme (27). These results indicate that the two tryptophans (W139 and W249) located closest to the active site (10) are not directly involved in halide binding, even though the fluorescence properties do change when halide is bound.

There was no significant change of fluorescence intensity when wild-type HheC was mixed with epoxide substrate (R)-PNSO in the absence of halide. Lutje Spelberg et al. (9) reported that HheC converted (R)-PNSO to the corresponding azido alcohol with high enantioselectivity, which indicates that it can bind to the wild-type enzyme, but apparently the binding does not influence the fluorescence properties. Other epoxides that can be converted but did not influence fluorescence included 5 mM (R)-epichlorohydrin, (R,S)-1,2-epoxybutane, and (R,S)-1,2-epoxypropane.

Quenching of Wild-Type HheC and Tryptophan Mutants by Acrylamide. Measurements of tryptophan fluorescence quenching by acrylamide are often used to obtain information about changes in the local environment of tryptophans upon ligand binding (29). For HheC, fluorescence quenching by acrylamide was measured in the absence and presence of 20 mM bromide. The Stern–Volmer plots of wild-type and mutant HheC enzymes were linear at acrylamide concentrations below 0.1 M but were slightly upward curved at a high concentration of acrylamide (Figure 3). This can be explained in terms of a static quenching component, which is due to a short distance between quencher and chromophore molecules at the moment that the latter becomes excited (29). The quenching constants (K_{sv}) were derived from the initial slopes of the corresponding Stern–Volmer plots (Table 3). The variation of the K_{sv} values reflects differences in the accessibility of tryptophan residues to solvent. Relatively exposed tryptophans give high K_{sv} constants, and replacement of these residues would consequently reduce the K_{sv} value.

Without substrate present, all HheC variants displayed a similar acrylamide quenching constant, suggesting that the acrylamide accessibilities of their fluorescent tryptophan residues are similar. As the fluorescence properties of the tryptophans in wild-type HheC cannot be separately studied in the native ligand-free state, no direct conclusions can be drawn about the effect of bromide on the local environment of each tryptophan residue. However, a comparison of the microenvironments of the tryptophans of the bromide-bound

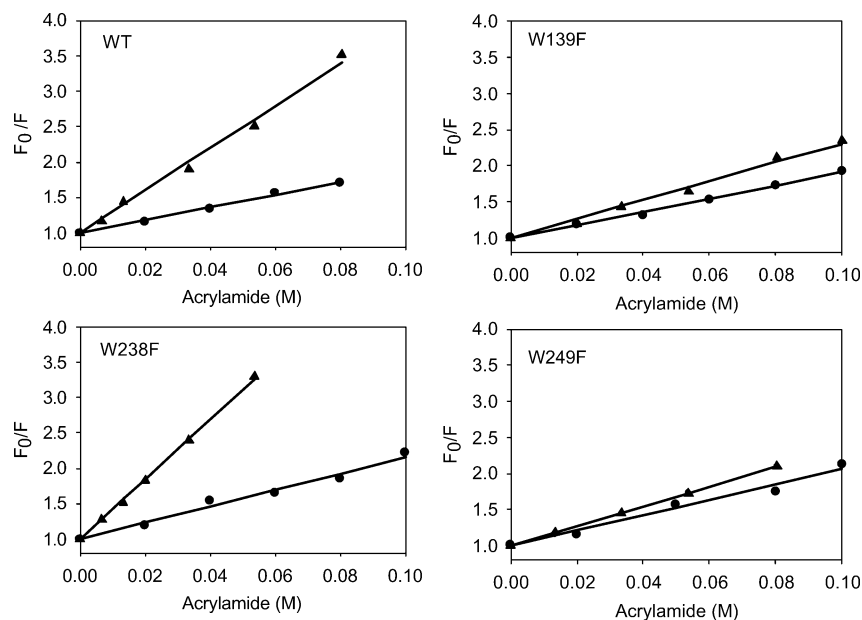


FIGURE 3: Stern–Volmer plots of fluorescence quenching by acrylamide. Measurements were done in the absence of substrate (●) or with 20 mM bromide (▲). The slopes of the best linear fit for each data set (K_{sv} values) are shown in Table 3.

enzyme can be made using the measured K_{sv} values. With 20 mM bromide, mutant W238F showed a K_{sv} value that is 1.4-fold higher than that of the wild-type enzyme, while the K_{sv} values of mutants W139F and W249F were 50–55% lower than that for wild-type HheC, suggesting that W238 is more buried and W139 and W249 are more exposed than the average tryptophans in HheC, which is consistent with the conclusion that was obtained from the λ_{Emax} measurement of those HheC variants in the presence of 20 mM bromide.

Effect of pH on Fluorescence Emission Intensity. To test if a charged amino acid residue acts as a quencher of tryptophan fluorescence in the native protein, we measured the pH dependence of the fluorescence emission intensity for the wild-type and mutant enzymes (Figure 4). It was found that the fluorescence of wild-type HheC and mutants W238F and W249F is higher at low pH than that at high pH with an apparent pK_a of 7, while the fluorescence emission intensities of mutant W139F changed very little in the pH range between 5.8 and 11. Moreover, the pH dependence of the fluorescence intensity for wild-type HheC disappeared in the presence of 20 mM bromide (Figure 4A). These results indicate that the fluorescence quenching due to W139 correlates with the deprotonated state of a group with a pK_a of about 7, for example, a histidine, and that this quenching process can also be suppressed by adding bromide.

To probe whether a histidine residue is responsible for the observed fluorescence quenching, DEPC, a histidine-specific reagent, was used. HheC contains seven histidine residues per subunit. In the presence of 1 mM DEPC, only one histidine was modified and the pH dependence of fluorescence still remained. The pH dependence of the fluorescence of wild-type HheC disappeared after the enzyme was incubated with 3 mM DEPC for 2 min. Under those conditions, the enzyme retained 90% of its activity compared to HheC without modification, suggesting that the modified enzyme is folded correctly. The fluorescence intensity in the pH range of 5.8–10 was similar to that of the native HheC

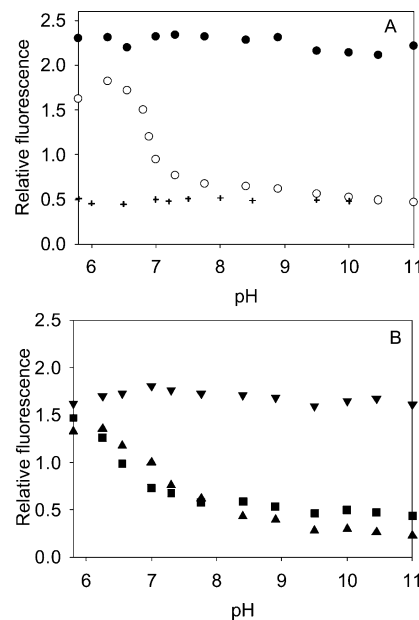


FIGURE 4: Effect of pH titration on the fluorescence of HheC variants. Panel A: wild-type HheC in the absence (○) and presence (●) of 20 mM bromide, and in the presence of 3 mM DEPC (+). Panel B: mutant W139F (▼), mutant W238F (■), and mutant W249F (▲) in the absence of bromide. The fluorescence was determined using a mixed buffer system of 50 mM Bis-Tris, Bis-Tris propane, and Caps containing 0.05 mg/mL protein.

at high pH (Figure 4A); i.e., the modified enzyme no longer showed the loss of W139-induced quenching at low pH. Spectrophotometric analysis revealed that three histidines had been modified. The structure of halide-bound HheC shows that H26 is the most exposed among the seven histidines, and that two histidines, H198 and H201, are relatively close to W139. Taken together, these results might indicate that the one that was modified at low concentration of DEPC is H26 and the latter two modified histidines might be H198 and H201, which play a crucial role in fluorescence quenching in the native state of HheC.

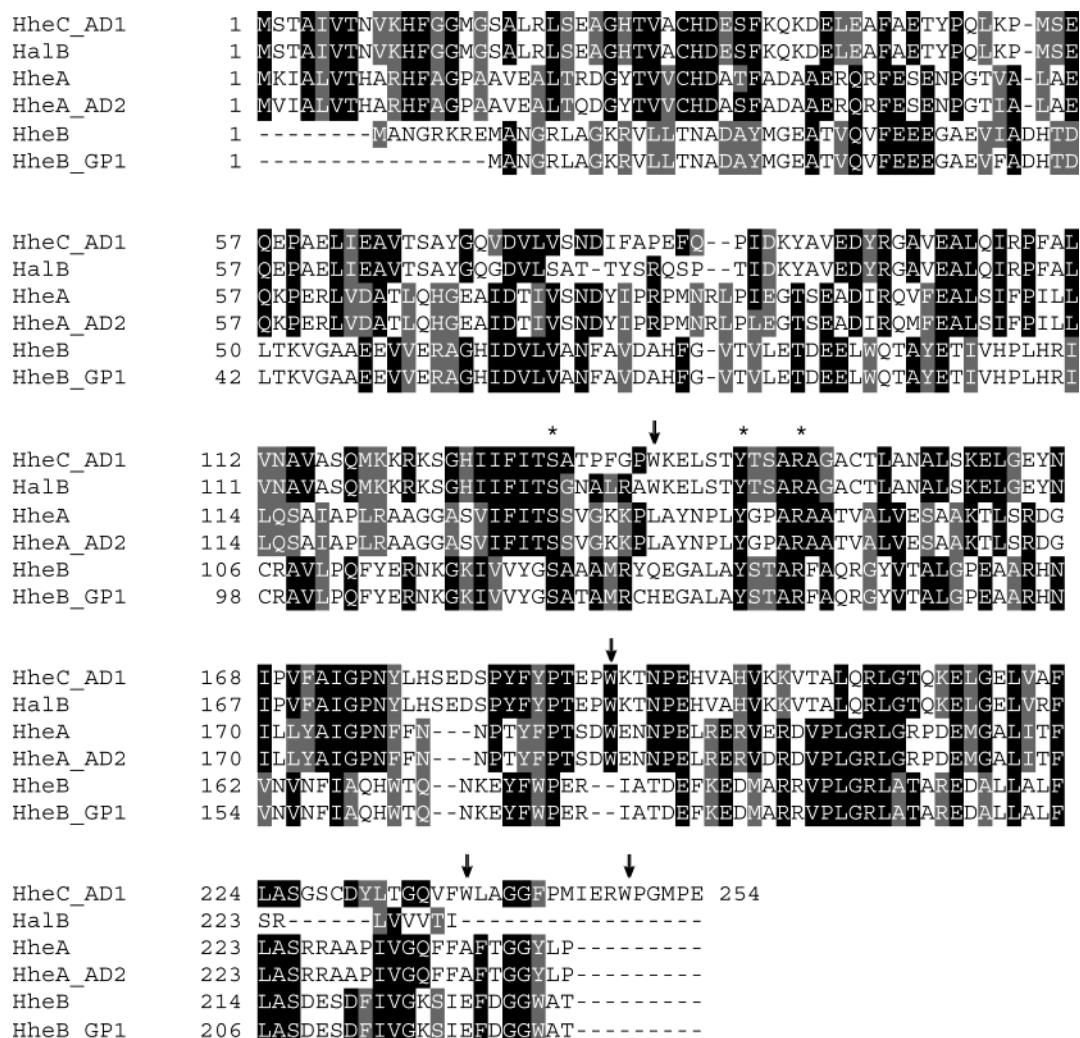


FIGURE 5: Sequence alignment of six haloalkane dehalogenases. The sequences were aligned by using the Clustal X program. The most conserved residues are marked in black. The active site residues are indicated with asterisks, and the tryptophan residues in HheC are indicated with arrows.

DISCUSSION

We used site-directed mutagenesis to probe the fluorescence properties and role in substrate binding of the individual tryptophan residues in HheC. Substitution of each of the tryptophan residues by phenylalanine, which is commonly used to replace tryptophan (30–34), resulted in three active mutants (W139F, W238F, and W249F) and one inactive mutant (W192F). Far-UV CD results indicate that all mutations, including mutant W192F, do not cause significant perturbations of the protein. Gel filtration experiments revealed that the impaired tetramerization of mutant W192F might be the main reason for its lack of activity, as it has been found that the tetramer is the active form of HheC (21). The X-ray structure of HheC shows that W192 is located in a hydrophobic cavity that is close to the interface of two subunits. Therefore, replacing W192 by a phenylalanine residue might destroy some interactions within the cavity, resulting in a change of the oligomeric state of HheC. Sequence alignment of all known haloalkane dehalogenases shows that W192 is the most conserved tryptophan residue (Figure 5), which suggests that W192 might be important for stabilizing the native structure of other haloalkane dehalogenases as well.

The steady-state kinetic studies with the mutants demonstrate that W139, W238, and W249 are not essential for catalysis. Mutating W238 does not cause a significant effect on the steady-state kinetics of HheC and the K_d value for halide, which is consistent with the observation that residue W238 is located far from the active site (10). With mutant W139F a large decrease in the K_m value was observed for (*S*)-PNSHH, while the K_m values for (*R*)-PNSHH and 1-dichloro-2-methyl-2-propanol were increased, suggesting that residue W139 might be even closer to the binding pocket of the aromatic group of (*S*)-PNSHH. (*S*)-PNSHH could not bind well to the active site of wild-type HheC, and the enzyme preferably converts (*R*)-PNSHH. This selectivity was lost by replacing W139 and resulted in a mutant (W139F) without any enantioselectivity toward PNSHH. It has been demonstrated that two other haloalkane dehalogenases, termed HheB-GP1 and HheA-AD2, display only a moderate enantioselectivity toward some aromatic haloalkanes (3, 9). Sequence alignment of haloalkane dehalogenases shows that W139 is not conserved in the other two types of haloalkane dehalogenases, which implies that mutations at the corresponding position in HheA and HheB may also influence the enantioselective properties of these enzymes since the predicted three-dimensional structures of those three halo-

hydrin dehalogenases closely resemble each other (3).

By mutating W249, the steady-state kinetics can be significantly altered with both aliphatic and aromatic halo-hydrins. However, W249 does not seem to be directly involved in halide binding since mutant W249F displays a K_d value for halide similar to that of wild-type HheC. Therefore, the changes of the K_m values with all tested substrates that occurred when W249 was replaced might be due to an effect on the R group of the substrates. Replacing W249 largely increased the k_{cat} value for (R)-PNSHH, which can be explained by enhancing the rate of bromide release in the catalytic cycle since this step was identified as rate-limiting (27). Therefore, W249 might be close to the halide export route or influence halide release indirectly.

Fluorescence measurements revealed a remarkable increase of the tryptophan fluorescence when halide is added to wild-type HheC. This unusual increase in fluorescence upon halide binding contrasts with what has been observed in haloalkane dehalogenase from *Xanthobacter autotrophicus* (DhlA), where halide binding results in a decrease of fluorescence intensity due to a direct interaction of halide with the two tryptophans that bind it (35). Furthermore, iodide is often used as a selective collisional fluorescence quencher to detect tryptophanyl side chains exposed to solvent (25). Thus, the increase of fluorescence intensity upon halide binding is probably not due to a direct interaction between halide and tryptophans.

A change in fluorescence intensity induced by ligand binding to a protein can also result from local conformational changes that alter the interactions of tryptophan residues with their neighboring groups (31, 36–40). To test this hypothesis, the fluorescence emission spectra of the HheC variants were studied. This revealed a low fluorescence yield of HheC in the native state, and W139 acts as an energy acceptor of one or more of the other tryptophans. W249 is the candidate for energy donor since the distance between those two tryptophan residues is only 4 Å. An internal quenching of tryptophan fluorescence in the native state was also observed in yeast 3-phosphoglycerate kinase (30, 41, 42).

The results support the possibility that the large increase of fluorescence in wild-type HheC when bromide is bound is due to a local conformational change around the active site, causing residue W139 and its quencher group to become separated. This motion would also suppress energy transfer from the other tryptophans to W139 and thereby enhance overall protein fluorescence. An attempt to crystallize HheC in the absence of halide has failed, indicating that significant differences may occur between the structures of free and ligand-bound enzyme. However, this also makes it impossible to directly observe which residues are involved in the proposed conformational change.

A histidine residue would be a candidate for such a group that is responsible for the fluorescence quenching of W139 since pH titration experiments revealed the involvement of an ionizable group with a pK_a of around 7, and two histidines (W198 and H201) are located close to W139 (10). A histidine residue cannot be protonated when it is chemically modified by DEPC. Indeed, the protonation event that led to loss of quenching at low pH no longer occurred when the DEPC-modified enzyme was titrated from pH 5.8 to pH 10 (Figure 4A). This suggests that the change of the microenvironment of W139 that occurs when bromide becomes bound and/or

when protonation takes place correlates with the protonation of a histidine residue. Normally, a protonated His residue is an efficient tryptophan fluorescence quencher (32, 39, 43). Thus, it is not likely that there is a direct interaction between a His residue and W139 since HheC shows a higher fluorescence intensity in the protonated form. Instead, protonation might induce a local conformational change that separates W139 and its quencher group. The quencher could be a protein residue that interacts with the His residue(s) that becomes protonated. Summarizing, the fluorescence quenching experiments suggest that bromide binding and protonation induce a local conformational change that separates W139 from its quencher group, by which the total intrinsic protein fluorescence of HheC is enhanced.

REFERENCES

1. Castro, C. E., and Bartnicki, E. W. (1968) Epoxidation of halo-hydrins, epoxide opening, and transhalogenation by a *Flavobacterium* sp., *Biochemistry* 7, 3213–3218.
2. Van den Wijngaard, A. J., Reuvekamp, P. T. W., and Janssen, D. B. (1991) Purification and characterization of haloalcohol dehalogenase from *Arthrobacter* sp. strain AD2, *J. Bacteriol.* 173, 124–129.
3. Van Hylckama Vlieg, J. E. T., Tang, L., Lutje Spelberg, J. H., Smilda, T., Poelarends, G. J., Bosma, T., van Merode, A. E. J., and Janssen, D. B. (2001) Halo-hydrin dehalogenases are structurally and mechanistically closely related to short-chain dehydrogenases/reductases, *J. Bacteriol.* 183, 5058–5066.
4. Assis, H. M. S., Sallis, P. J., Bull, A. T., and Hardman, D. J. (1998) Biochemical characterization of a haloalcohol dehalogenase from *Arthrobacter erythrii* H10a, *Enzyme Microb. Technol.* 22, 568–574.
5. Nakamura, T., Nagasawa, T., Yu, F., Wanatabe, I., and Yamada, H. (1994) Characterization of a novel enantioselective halo-hydrin-hydrogen lyase, *Appl. Environ. Microbiol.* 60, 1297–1301.
6. Nakamura, T., Nagasawa, T., Yu, F., Watanabe, I., and Yamada, H. (1991) A new catalytic function of halo-hydrin hydrogen-halide-lyase, synthesis of β -hydroxynitriles from epoxides and cyanide, *Biochem. Biophys. Res. Commun.* 180, 124–130.
7. Van den Wijngaard, A. J., Janssen, D. B., and Witholt, B. (1989) Degradation of epichlorohydrin and halo-hydrins by bacteria isolated from freshwater sediment, *J. Gen. Microbiol.* 135, 2199–2208.
8. Lutje Spelberg, J. H., van Hylckama Vlieg, J. E. T., Bosma, T., Kellogg, R. M., and Janssen, D. B. (1999) A tandem enzyme reaction to produce optically active halo-hydrins, epoxides and diols, *Tetrahedron: Asymmetry* 10, 2863–2870.
9. Lutje Spelberg, J. H., van Hylckama Vlieg, J. E. T., Tang, L., Janssen, D. B., and Kellogg, R. M. (2001) Highly enantioselective and regioselective biocatalytic azidolysis of aromatic epoxides, *Org. Lett.* 3, 41–43.
10. de Jong, R. M., Tiesinga, J. J. W., Rozeboom, H. J., Kalk, K. H., Tang, L., Janssen, D. B., and Dijkstra, B. W. (2003) Structure and mechanism of a bacterial haloalcohol dehalogenase: a new variation of the short-chain dehydrogenase/reductase fold without an NAD(P)H binding site, *EMBO J.* 22, 4933–4944.
11. Newman, J., Peat, T. S., Richard, R., Kan, L., Swanson, P. E., Affholter, J. A., Holmes, I. H., Schindler, J. F., Unkefer, C. J., and Terwilliger, T. C. (1999) Haloalkane dehalogenases: structure of a *Rhodococcus* enzyme, *Biochemistry* 38, 16105–16114.
12. Yang, G., Liu, R. Q., Taylor, K. L., Xiang, H., Price, J., and Dunaway-Mariano, D. (1996) Identification of active site residues essential to 4-chlorobenzoyl-coenzyme A dehalogenase catalysis by chemical modification and site directed mutagenesis, *Biochemistry* 35, 10879–10885.
13. Tzeng, H. F., Laughlin, L. T., and Armstrong, R. N. (1998) Semifunctional site-specific mutants affecting the hydrolytic half-reaction of microsomal epoxide hydrolase, *Biochemistry* 37, 2905–2911.
14. Nardini, M., Ridder, I. S., Rozeboom, H. J., Kalk, K. H., Rink, R., Janssen, D. B., and Dijkstra, B. W. (1999) The X-ray structure of epoxide hydrolase from *Agrobacterium radiobacter* AD1: an enzyme to detoxify harmful epoxides, *J. Biol. Chem.* 274, 14579–14586.

15. Rink, R., and Janssen, D. B. (1998) Kinetic mechanism of the enantioselective conversion of styrene oxide by epoxide hydrolase from *Agrobacterium radiobacter* AD1, *Biochemistry* 37, 18119–18127.
16. Kennes, C., Pries, F., Krooshof, G. H., Bokma, E., Kingma, J., and Janssen, D. B. (1995) Replacement of tryptophan residues in haloalkane dehalogenase reduces halide binding and catalytic activity, *Eur. J. Biochem.* 228, 403–407.
17. Bennett, M. J., Schlegel, B. P., Jez, J. M., Penning, T. M., and Lewis, M. (1996) Structure of 3 α -hydroxysteroid/dihydrodiol dehydrogenase complexes with NADP⁺, *Biochemistry* 35, 10702–10711.
18. Jez, J. M., Schlegel, B. P., and Penning, T. M. (1996) Characterization of the substrate binding site in rat liver 3 α -hydroxysteroid/dihydrodiol dehydrogenase, *J. Biol. Chem.* 271, 30190–30198.
19. Westkaemper, R. B., and Hanzlik, R. P. (1981) Mechanistic studies of epoxide hydrolase utilizing a continuous spectrophotometric assay, *Arch. Biochem. Biophys.* 208, 195–204.
20. Rink, R., Fennema, M., Smids, M., Dehmel, U., and Janssen, D. B. (1997) Primary structure and catalytic mechanism of epoxide hydrolase from *Agrobacterium radiobacter* AD1, *J. Biol. Chem.* 272, 14650–14657.
21. Tang, L., Van Hylckama Vlieg, J. E. T., Lutje Spelberg, J., Fraaije, M. W., and Janssen, D. B. (2002) Improved stability of halohydrin dehalogenase from *Agrobacterium radiobacter* AD1 by replacement of cysteine residues, *Enzyme Microb. Technol.* 30, 251–258.
22. Bergmann, J. G., and Sanik, J. (1957) Determination of trace amounts of chlorine in naphtha, *Anal. Chem.* 29, 241–243.
23. Lutje Spelberg, J. H., Tang, L., van Gelder, M., Kellogg, R. M., and Janssen, D. B. (2002) Exploration of the biocatalytic potential of a halohydrin dehalogenase using chromogenic substrates, *Tetrahedron: Asymmetry* 13, 1083–1089.
24. Eisinger, J. (1969) A variable temperature, U.V. luminescence spectrograph for small samples, *Photochem. Photobiol.* 9, 247–258.
25. Eftink, M. R., and Ghiron, C. A. (1981) Fluorescence quenching studies with proteins, *Anal. Biochem.* 114, 199–227.
26. Miles, E. W. (1977) Modification of histidyl residues in proteins by diethyl pyrocarbonate, *Methods Enzymol.* 47, 431–442.
27. Tang, L., Lutje Spelberg, J. H., Fraaije, M. W., and Janssen, D. B. (2003) Kinetic mechanism and enantioselectivity of halohydrin dehalogenase from *Agrobacterium radiobacter*, *Biochemistry* 42, 5378–5386.
28. Brustein, E. A., Vedenkina, N. S., and Ivkova, M. N. (1973) Fluorescence and the location of tryptophan residues in protein molecules, *Photochem. Photobiol.* 18, 263–279.
29. Eftink, M. R., and Ghiron, C. A. (1976) Exposure of tryptophanyl residues in proteins. Quantitative determination by fluorescence quenching studies, *Biochemistry* 15, 672–680.
30. Szpikowska, B. K., Beechem, J. M., Sherman, M. A., and Mas, M. T. (1994) Equilibrium unfolding of yeast phosphoglycerate kinase and its mutants lacking one or both native tryptophans: A circular dichroism and steady-state and time-resolved fluorescence study, *Biochemistry* 33, 2217–2225.
31. Beattie, B. K., and Merrill, A. R. (1999) A fluorescence investigation of the active site of *Pseudomonas aeruginosa* exotoxin A, *J. Biol. Chem.* 274, 15646–15654.
32. Martensson, L. G., Jonasson, P., Freskgard, P. O., Svensson, M., Carlsson, U., and Jonsson, B. H. (1995) Contribution of individual tryptophan residues to the fluorescence spectrum of native and denatured forms of human carbonic anhydrase II, *Biochemistry* 34, 1011–1021.
33. Nishimura, J. S., Mann, C. J., Ybarra, J., Mitchell, T., and Horowitz, P. M. (1990) Intrinsic fluorescence of succinyl-CoA synthetase and four tryptophan mutants. Tryptophan 76 and tryptophan 248 of the β -subunit are responsive to CoA binding, *Biochemistry* 29, 862–865.
34. Knappskog, P. M., and Haavik, J. (1995) Tryptophan fluorescence of human phenylalanine hydroxylase produced in *Escherichia coli*, *Biochemistry* 34, 11790–11799.
35. Schanstra, J. P., and Janssen, D. B. (1996) Kinetics of halide release of haloalkane dehalogenase: evidence for a slow conformational change, *Biochemistry* 35, 5624–5632.
36. Higashijima, T., Ferguson, K. M., Sternweis, P. C., and Ross, E. M. (1987) The effect of activating ligands on the intrinsic fluorescence of guanine nucleotide-binding regulatory proteins, *J. Biol. Chem.* 262, 752–756.
37. Pawagi, A. B., and Deber, C. M. (1990) Ligand-dependent quenching of tryptophan fluorescence in human erythrocyte hexose transport protein, *Biochemistry* 29, 950–955.
38. Deville-Bonne, D., Sellam, O., Merola, F., Lascu, I., Desmadril, M., and Veron, M. (1996) Phosphorylation of nucleoside diphosphate kinase at the active site studied by steady-state and time-resolved fluorescence, *Biochemistry* 35, 14643–14650.
39. Surarit, R., and Svasti, J. (1980) Effect of ligand binding on the conformation of human plasma vitamin D binding protein (group-specific component), *Biochem. J.* 191, 401–410.
40. Li, J., Szittner, R., and Meighen, E. A. (1998) Tryptophan fluorescence of the lux-specific *Vibrio harveyi* acyl-ACP thioesterase and its tryptophan mutants: structural properties and ligand-induced conformational change, *Biochemistry* 37, 16130–16138.
41. Nojima, H., Ikai, A., and Noda, H. (1976) Anomalous fluorescence of yeast 3-phosphoglycerate kinase, *Biochim. Biophys. Acta* 427, 20–27.
42. Nojima, H., Ikai, A., Oshima, T., and Noda, H. (1977) Reversible thermal unfolding of thermostable phosphoglycerate kinase. Thermostability associated with mean zero enthalpy change, *J. Mol. Biol.* 116, 429–442.
43. Loewenthal, R., Sancho, J., and Fersht, A. R. (1991) Fluorescence spectrum of barnase: contributions of three tryptophan residues and a histidine-related pH dependence, *Biochemistry* 30, 6775–6779.

BI034941A